Journal of Ceramic Processing Research. Vol. 25, No. 5, pp. 751~759 (2024)
(Received 24 April 2024, Received in revised form 3 June 2024, Accepted 5 July 2024)
https://doi.org/10.36410/jcpr.2024.25.5.751

J O U R N A L O F
Ceramic Processing Research

Effects of polyacrylic acid-based binder on electrical property of potassium-sodium niobate ceramic

Jinjin Lin[a], Jiaxin Duan[a], Jiahao Huang[a], Ya Yang[a], Mingxing An[b], Zhiming Gao[c] and Yuanyu Wang[a,b,c,*]
[a]*College of Materials and Metallurgy, Guizhou University, Guizhou 550025, China*
[b]*Yasusa Chemical Co., Ltd., Jiaxing, Zhejiang 314200, China*
[c]*School of Materials Science and Engineering, Tianjin University, Tianjin 300072, China*

The Binder is of importance in the ceramic industry and polyacrylic acid (PAA) is a promising binder due to its low cost, and enhancement effect on the density and properties of the potassium-sodium niobate (KNN) ceramic. In this work, alkalescent, acidulous, and neutral PAA-based binders are investigated. The results suggest that the alkalescent and neutral PAA-based binders are conducive to the ceramic density. Except for the as-calcinated powder granulated by PAA-HPMC and PAA-C=CH$_2$, the values of median particle diameter (D50) for other powders are around 0.771 μm-0.863 μm, and corresponding cumulative distribution of D50 within the variation range of 50.05%-57.62% is detected. On the whole, the KNN ceramic synthesized by the AcPAA possesses the best combination properties with piezoelectric constant d_{33}~108 pC/N, and the breakdown strength E_b~3.93 kV/cm is obtained for PAA-DM, which is ascribed to the synergistic effect of granulated grain size and thermal behavior of the binders.

Keywords: Potassium-sodium niobate, Polyacrylic acid, Binder, Electrical property.

Introduction

In industry, polyacrylic acid [1] (PAA) is widely used in textiles, papermaking, construction, pharmaceuticals, and health and environmental protection [2, 3]. PAA can also be copolymerized with other monomers to form different functional polymers, these materials can be used to prepare polymer hydrogels [4], pressure-sensitive adhesives [5], ion exchange resins [6], ultra-high molecular weight polymers [7] and so on, with broad and far-reaching application prospects [8].

The use of PAA and its derivatives in the preparation of ceramic slurries is well-established [9]. PAA-based binders can improve the mechanical properties, sintered density, and composition uniformity of ceramic bodies [10], playing an important role in enhancing the overall performance of ceramics. The low thermal decomposition temperature of PAA [11] makes it easy to completely decompose during the de-bonding process of ceramics [12], with minimal residue, reducing impurities introduced. By using various modification techniques to control the mechanical and chemical properties of the binding phase, the effectiveness of the binder can be further enhanced.

Research has shown that PAA-based binders can increase the strength of ceramics at low concentrations (<5.0 vol%) [13], leading to uniform density and composition of the ceramics. For example, with only 2.5 vol% of PAA-based binder, the strength of oxides like SiO_2, TiO_2, and Al_2O_3 can be increased by at least 8 times, with the strength of Al_2O_3 increasing by about 24 times (0.3 to 7.6 MPa). Furthermore, the addition of a PAA-based binder improves the toughness of ceramic, with SiO_2 increasing by up to 2.8×10^{-3}~4.4×10^{-2} MPa·m$^{1/2}$ [14]. Compared to polyvinyl alcohol (PVA), PAA-based binders exhibit more uniform distribution, lower particle yield stress, and smaller inter-particle gaps, resulting in a more homogeneous internal structure in green bodies and ceramics [15].

Piezoelectric ceramics are widely used functional materials [16] that can convert mechanical energy into electrical energy and vice versa [17]. Lead-free piezoelectric ceramics are also known as environmentally coordinated piezoelectric ceramics. In many lead-free piezoelectric ceramics systems, potassium-sodium niobate ($K_{0.5}Na_{0.5}NbO_3$, KNN) ceramics with perovskite structure [18], good electric properties and high Curie temperature is believed to be promising candidates to replace lead based piezoelectric ceramics in the field of national defense, aerospace, communication, and other electronic devices [19]. The issue associated with lead-free KNN-based piezoelectric ceramics [20-22] is their poor sintering properties and low density [23], which makes it challenging to improve their electrical properties. Doping can be used to address this, but the complexity

*Corresponding author:
Tel : +86 13985175871
Fax: +86 13985175871
E-mail: yuanyuwang0216@163.com

of dopant systems leads to poor reproducibility and stability. Advanced preparation technologies that can significantly improve ceramic performance also incur higher production costs [24]. Instead of these approaches, modifying the use of binders to achieve improved sintering properties can significantly enhance the performance of ceramics by reducing defects incurred during sintering [25], making it a cost-effective and efficient alternative for industrialization. However, research on PAA-based binders and their effects in enhancing KNN-based ceramic properties is limited, since the raw materials to prepare the KNN consist of hetero-charges and contain a variety of non-equivalent ions, so the pH range is wide and the particles are seriously agglomerated. Therefore, the modification of PAA or its functional groups can decrease the hetero-charges in the granulation process and is conducive to enhancing the powder granulation.

Therefore, this work focuses on synthesizing modified PAA-based binders to prepare KNN-based ceramic, studying the influence of binders on ceramic sintering and associated electrical properties, and elucidating the mechanism. Binder modification is the key to enhancing the sintering and electrical properties of KNN-based ceramics. The functional group of polyacrylic acid (PAA) is the carboxyl group (-COOH), and its dissociation reaction is $R\text{-}COOH+H_2O—R\text{-}COO^-+ H_3O^+$. With the increase of pH value (4.5-5), the negatively charged carboxylic acid group (COO^-) formed by dissociation will be combined with K, Na, and Nb ions in KNN, and the powder is attracted by electrostatic gravity to gather each other, so the bonding effect is good. However, if the amount of COO^- is too large, the granulation particle size becomes larger, and the particle fluidity becomes worse, leading to uneven granulation. In addition, electrically neutral polymers or functional groups that are not sensitive to changes in pH value or ion concentration can shield the potential layer generated by the partially ionized PAA skeleton, reducing agglomeration and controlling particle size. KNN mixed raw materials are in the hetero-charge region and contain many kinds of unequal ions, so the pH range is wide and the particles are seriously agglomerated. Therefore, the modification of the PAA functional group can narrow the heterocharge region in the granulation process, which is also conducive to enhancing the granulation effect of ceramic powder. Therefore, in this work, the density and electrical properties of the KNN ceramics are investigated by adjusting the acidity and alkalinity of modified PAA adopting solution polymerization, mixed neutral polymer, copolymerization, graft modification, and other means.

Experiments

$K_{0.5}Na_{0.5}NbO_3$ (KNN) ceramics [26] were synthesized via a solid-state method [27] using modified PAA. High-purity raw materials obtained from Sinopharm Chemical Reagent Co., Ltd., CN. The raw materials used were K_2CO_3 (99%), Na_2CO_3 (99.8%), Nb_2O_5 (99.5%). The stoichiometrically proportioned raw material powders [28] were ground in a planetary ball mill using ZrO_2 balls [29] and absolute ethanol for 12 hours. The resulting slurry was dried, calcined at 850 °C in air for 6 hours, and then milled again for 12 hours [30]. The dried slurry obtained from the secondary ball milling was ground into a fine powder and mixed with various PAA-based binders to form granules and the corresponding products are listed in Table 1. The granules were then pressed into disks with a diameter of 12 mm. Finally, the samples were sintered in covered alumina crucibles at a temperature range of 1080-1110 °C for 5 hours [31].

To ensure the purity and homogeneity of the final KNN ceramic samples, we used the same raw materials, calculated the quality of raw materials accurately, ensured that the grinding time and the speed were consistent for all samples, and finally customized the sintering conditions of each sample to guarantee the quality.

X-ray diffraction (XRD) using Cu$K\alpha$ radiation was performed on the D8 Advanced Diffractometer to analyze the phase structures of the ceramics. The Zeiss Sigma 300 was utilized to obtain scanning electron microscopy (SEM) images for microstructure analysis, while the dielectric properties and impedance spectrum were determined using an LCR analyzer (E4991A,

Table 1-1. Nominal alkalescent binders.

Modified binder	Abbreviation	Volume ratio	Wight ratio
PAA adjusted by diethylaminoacetaldehyde methacrylate (DM)	PAA-DM	0.5:1	
PAA diluted by alkalescent sodium polyacrylate (APAANa)	PAA-APAANa	0.5:1	

Table 1-2. Nominal acidulous binders.

Modified binder	Abbreviation	Volume ratio	Wight ratio
PAA adjusted by nonpolar sodium polyacrylate (PAANa)	PAA-PAANa		0.5:1
PAA adjusted by nonionic polyacrylamide (PAM)	PAA-PAM		0.5:1
PAA adjusted by citric acid and sodium citrate (10 mmol/L) buffer	AcPAA		0.5:1

Table 1-3. Nominal neutral binders.

Modified binder	Abbreviation	Volume ratio	Wight ratio
PAA mixed with neutral hydroxypropyl methylcelluloe (HPMC)	PAA-HPMC	0.2:0.8	
PAA with partial hydroxyl group transferring to ethylene-ethylene (-C=CH_2)	PAA-C=CH_2	0.2:0.8	
PAA mixed with 2-ethylhexyl acrylate (2-EHA)	PAA-2-EHA	0.5:1	
Sodium polyacrylate (PAANa)	PAANa		

Agilent, USA). The grain size distribution was measured with a Baibaxter laser particle size analyzer (BT-9300S, Dandong). An impedance analyzer (WK6500P/B, Sanqi Electronic Technology Limited Company, Changsha) was used to measure the complex impedance data of ceramics and then calculated the conductivity, dielectric constant, and dielectric loss of ceramics. The piezoelectric analyzer (ZJ-6A, Institute of Acoustics, CAS) was used to measure the piezoelectric coefficient and voltage strain relationship of ceramics. The density analyzer (MH-120C, Meida Instrument Equipment Limited Company, Shenzhen) was used to measure the substance density, and the viscosity of ceramic fluid was measured with the viscosity analyzer (NDJ-5S, Jinghui Instrument Equipment Limited Company, Shanghai).

Results and Discussion

Shrinking percentage, density of samples, and electrical properties

Fig. 1(a) is the shrinking percentage and density of the samples synthesized by different modified binders. It is found that the PAA-DM, PAA-HPMC, and PAA-2-EHA are positive for the shrinking of KNN as-sintered ceramic. On the contrary, the PAANa leads to the smallest shrinkage. A similar change is observed in the density of the ceramics. The results indicate that the alkalescent group, i.e. -NH_2, is superior to the alkalescent environment since the ceramic prepared by the PAA-APAANa is shrunk lesser. Moreover, the small molecular weight (MW) of the binder, for example, PAANa, is adverse to the bonding effect, resulting in the poor shrinkage and density of the ceramic. In contrast, the acidulous binder, such as PAA-PAANa, PAA-PAM, and AcPAA which is buffered with citrate buffer solution, has a small influence on the shrinkage but positively affects the density of the KNN ceramic.

Fig. 1(b) gives the piezoelectric constant (d_{33}) and breakdown strength (E_b) of the samples. It is observed that the ceramic synthesized by the PAA-APAANa or AcPAA, possesses the highest d_{33} of 103 or 108 pC/N, while the smallest d_{33} is detected in the ceramic by PAANa, probably resulting from poor density. The maximum d_{33} for PAA-APAANa or AcPAA is ascribed to the decrease of the carboxylic acid group (-COO^-) through the regulation of pH. The breakdown strength is also investigated, as shown in Fig. 2. It is found that the highest E_b of 3.93 kV/mm and 3.73 kV/mm are obtained in the ceramics by PAA-DM and PAA-2-EHA. It's worth noting that the DM and 2-EHA possess the neutral diethyl (-C=CH_2) and ester (-COO^-) groups, which shields the electrostatic attraction of -COO^- to the K^+ and Na^+ and consequently reduces the particle aggregation which could be deteriorating the performances of the ceramic. Besides, the lowest d_{33} and E_b are obtained simultaneously in the ceramic fabricated by PAANa. That is also probably because of the poorest density.

Viscosity and characterization of granulated powder

The viscosity of the binders is presented in Fig. 3.

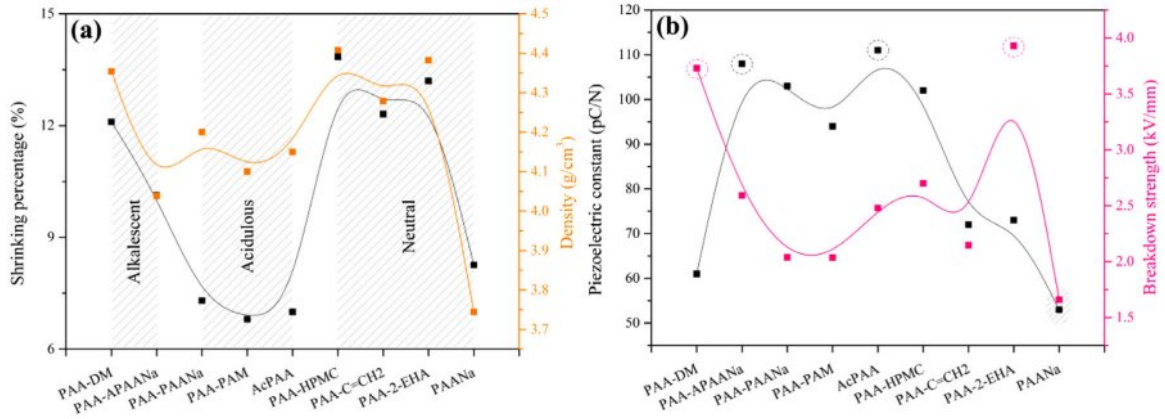

Fig. 1. (a) Shrinking percentage and density of the samples synthesized by different modified binders, (b) Piezoelectric constant and breakdown strength of the samples.

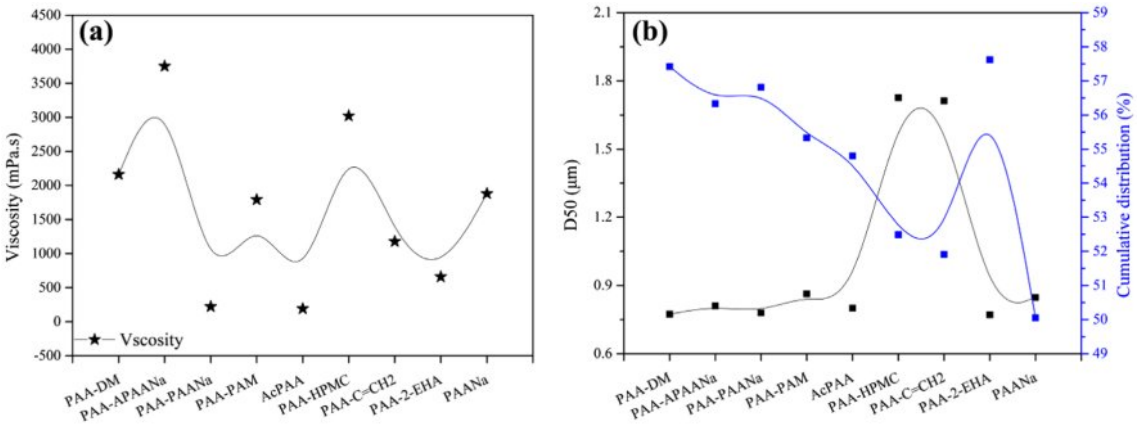

Fig. 2. (a) Viscosity of the binders, (b) Median particle diameter (D50) and cumulative distribution of the powder after granulation.

It is seen that the PAA-APAANa possesses the highest viscosity while the viscosity of PAA-PAANa is the lowest. The reason for the highest viscosity of PAA-APAANa is probably because the PAANa treated with ammonia water gives birth to flocculation. Interestingly, such flocculation doesn't affect the binding effect which plays an indispensable role in enhanced electrical properties.

Fig. 2(b) is the median particle diameter (D50) and cumulative distribution of the powder after granulation. It is found that except for the powder granulated by PAA-HPMC and PAA-C=CH_2, the values of D50 for other powders are around 0.771 μm-0.863 μm, and the corresponding cumulative distribution of D50 within the variation range of 50.05%-57.62% is detected. For PAA-HPMC and PAA-C=CH_2, the size of the particles is

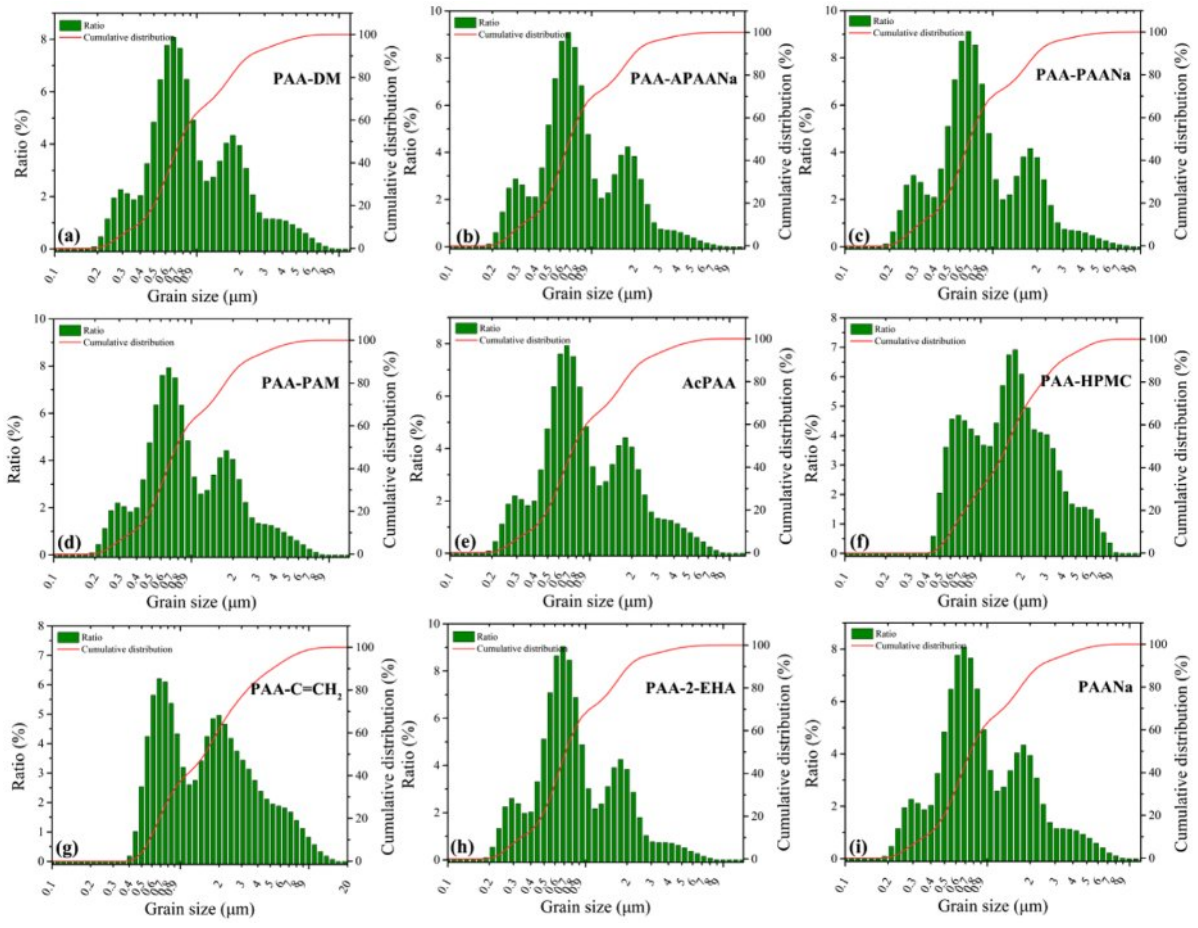

Fig. 3. Particle size distribution of the powders after granulation for different binders.

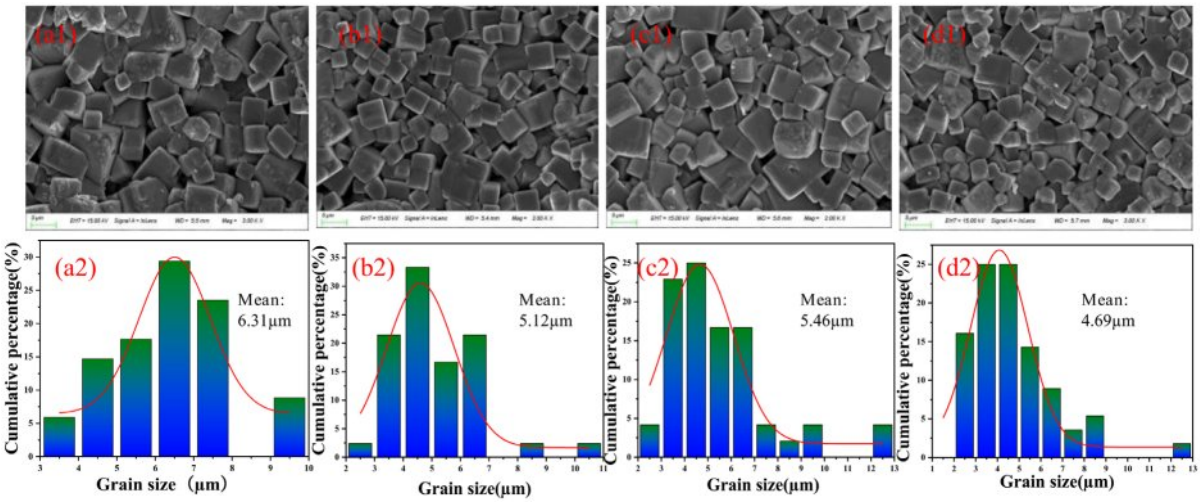

Fig. 4. Surface morphology and their corresponding grain size distribution of the ceramics synthesized by (a) PAA-DM, (b) PAA-PAM, (c) PAA-HPMC, (d) PAA-2-EHA.

about two times larger than the others, probably because in the two binders, it is still reflected as the electrostatic effect of COO^- in PAA.

Fig. 3 is the particle size distribution of the powders after granulation for different binders. As can be seen, except for the powders granulated by PAA-HPMC and PAA-C=CH_2, the others present quasi-normal distribution, probably owing to the COO^- which is not changed in the two binders.

To investigate the effects of particle size distribution on the microstructure of the ceramics, the surface morphology and their corresponding grain size distribution of the ceramics synthesized by the PAA-DM, PAA-PAM, PAA-HPMC and PAA-2-EHA, and their corresponding grain size distribution, are presented in Fig. 4. It is seen that the samples consist of the grains with appreciate size and the small and big grains are normally distributed for PAA-PAM, PAA-HPMC and PAA-2-EHA. However, the grain size distribution of PAA-DM is more uniform. The results indicate that the size distribution of the granulated powders with different binders has little influence on the grain size of the as-sintered ceramics. Moreover, combined with the samples' density, the densification of the ceramics is thought to be related to many factors, besides a quasi-normal size distribution which is acknowledged to facilitate the ceramic densification through the filling of interspace induced by big particles with the small ones. The results are also demonstrated by the grain size distribution of the corresponding ceramics, as shown in Figs. 4(a2)-(d2).

Complex impedance spectra

Fig. 5 gives the complex impedance spectra of the ceramics measured at different temperatures and the frequencies ranging from 100 Hz to 1 MHz. The fitting circuits are also exhibited in the figures. It is detected that all samples present a circular arc pattern, demonstrating that the samples possess single-grain polarization behavior.

As can be seen, the resistance of the sample decreases gradually with temperature, leading to a decrease in sample insulation. Also, the resistance of the ceramic by PAANa is much lower than the others, agreeing with the low density. No other polarization, such as space-charge polarization caused by pores, is detected, indicating that there are fewer pores in the ceramics.

Fig. 6(a) is the activation energy (E_a) based on the $Z' \sim Z''$ curves, and the E_a can be evaluated by the Arrhenius equation:

$$\omega = \omega_0 \exp(-E_a/k_B T) \quad (1)$$

Where ω_0, k_B, and T are the pre-exponential factor, Boltzmann constant, and absolute temperature, respectively. According to the calculated results, it can be inferred that the relaxation polarization in the ceramics originated from the oxygen vacancy migration in the grains since the E_a for oxygen-vacancy migration is approximately 1 eV according to the theoretical calculation of the ionic transport in perovskite oxides. To observe the relaxation time τ, the equation $2\pi f\tau=1$ is employed using the $Z' \sim Z''$ curve at 500 °C, 550 °C, and 600 °C, where f corresponds to the frequency at the arc maximum. The E_a and τ are exhibited in Fig. 6(b). The maximum E_a and minimum τ are observed for PAA-DM and PAA-2-EHA while the minimum E_a and τ are detected for PAANa, which means the ceramic synthesized by PAANa possesses strong oxygen-vacancy migration, leading to big leakage current and poor d_{33}, as discussed above.

Thermal analysis

For investigation of the removal process, the thermal

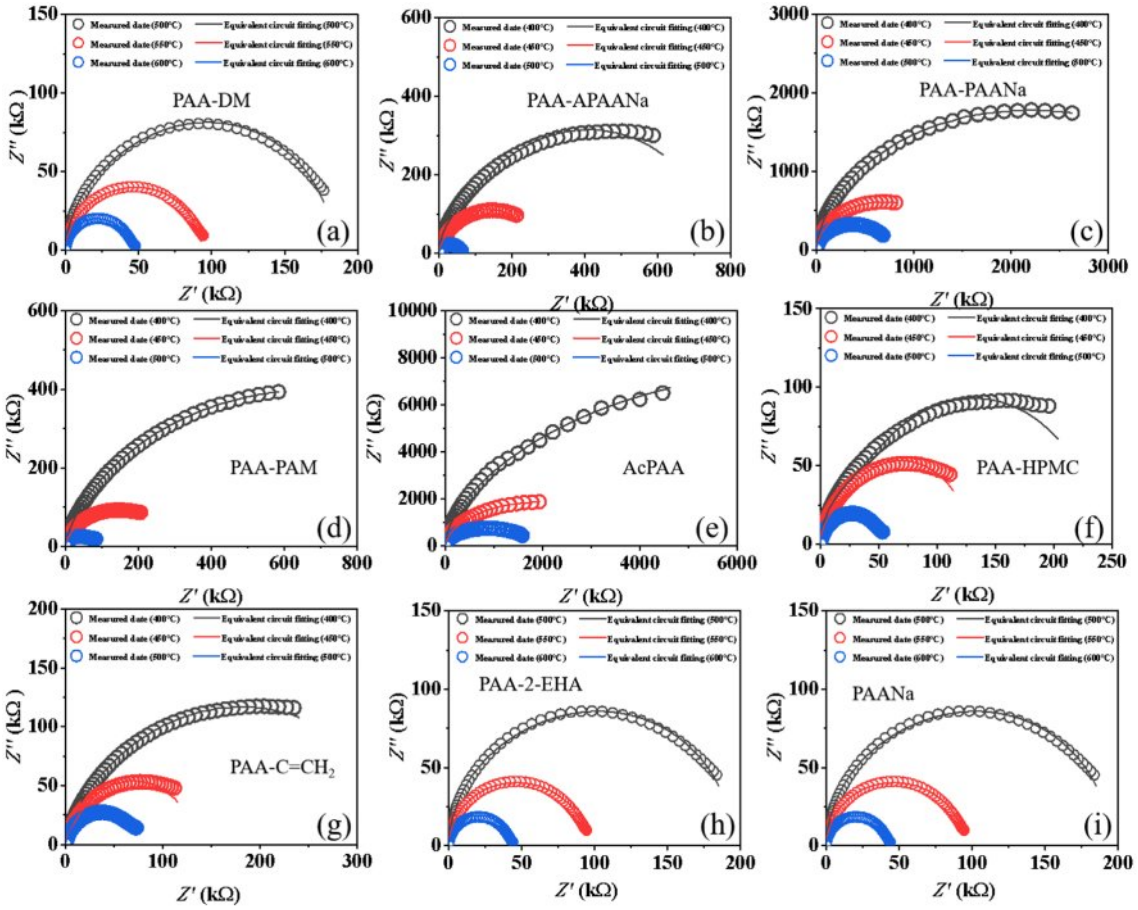

Fig. 5. Complex impedance spectra of the ceramics.

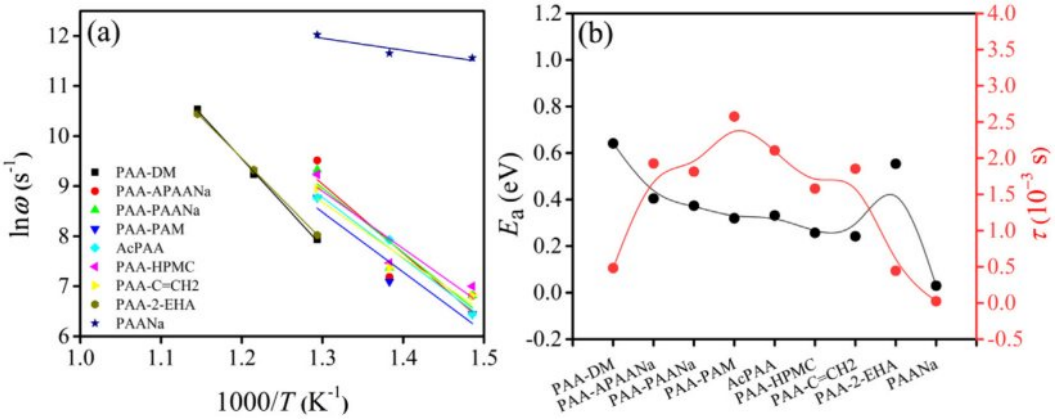

Fig. 6. (a) Activation energy E_a, (b) Relaxation time of the samples.

analysis of the PAA and PAANa is presented in Fig. 7. As can be seen, the removal of PAA happens in the temperature range of ~88 °C since the thermogravimetric (TG) analysis and the derivative thermogravimetry (DTG) appear to sharply change. By contrast, the temperature range of removal for PAANa is ~56 °C. Furthermore, the ending of the removal is 271 °C for PAA, lower than that of PAANa (307 °C). Generally speaking, the low beginning temperature and wide temperature range for the removal are conducive to the complete binder removal. Therefore, according to Fig. 7, the PAA-APAANa, PAA-PAANa, AcPAA, and PAA-HPMC binders display improved binding effect which generates increased comprehensive performances of the as-sintered ceramics using them as binders to some extent.

Mechanism analysis

The comprehensive performances of the binders and

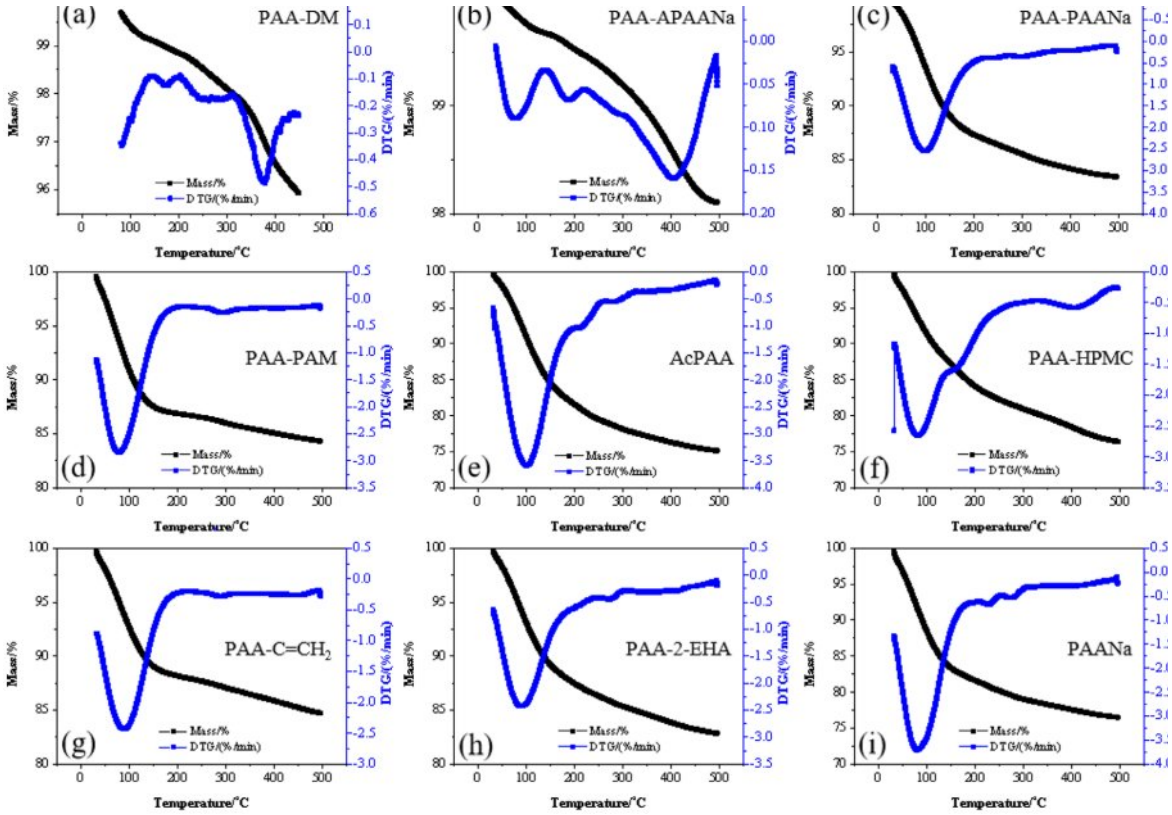

Fig. 7. Thermal analysis of the binders.

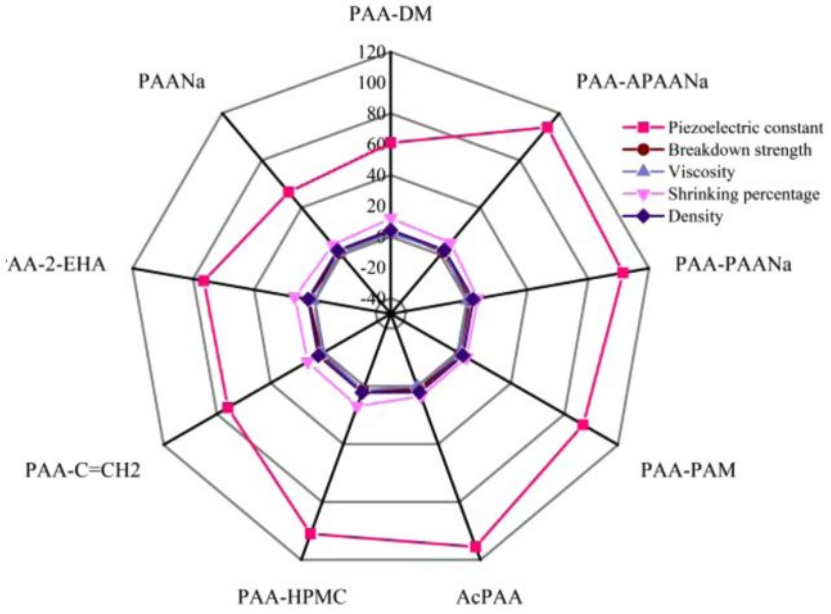

Fig. 8. (a) The comprehensive performances of the binders and the as-sintered ceramics using them.

the as-sintered ceramics using them are exhibited in Fig. 8(a). It is found that the viscosity has influenced the shrinkage and density of the as-sintered ceramics, but there is no direct relation between the shrinkage or density and electrical performances of the ceramics. As seen in Fig. 8(a), the optimized piezoelectric constants are obtained in alkalescent PAA-APAANa and acidulous AcPAA while the maximum breakdown strengths are observed in alkalescent PAA-DM and neutral PAA-2-EHA.

Table 2-1. Nominal alkalescent binders.

Modified binder	Structural formulas	Active functional groups
PAA-DM	$CH_2=C(CH_3)COOCH_2CH_2N(C_2H_5)(CH_2CH_2OH)CH_3$	$CH_2=C(CH_3)COO\text{-}CH_2CH_2N(C_2H_5)\text{-}(CH_2CH_2OH)CH_3\text{-}$
PAA-APAANa	$[\text{-}CH_2\text{-}CH(CO_2Na)\text{-}]n$	$\text{-}CO_2Na$

Table 2-2. Nominal acidulous binders

Modified binder	Structural formulas	Active functional groups
PAA-PAANa	$[\text{-}CH_2\text{-}CH(CO_2Na)\text{-}]n$	$\text{-}CO_2Na$
PAA-PAM	$[\text{-}CH_2\text{-}CH(CONH_2)\text{-}]n$	$\text{-}CONH_2$
AcPAA	$HOC(CH_2COOH)_2COOH\ Na_3C_6H_5O_7$	-COOH, -OH

Table 2-3. Nominal neutral binders.

Modified binder	Structural formulas	Active functional groups
PAA-HPMC	$[\text{-}OCH_3\text{-}CH(OH)CH_2O\text{-}]n$	$\text{-}OCH_3$
PAA-C=CH_2	$CH_2=CH_2$	$\text{-}C=CH_2$
PAA-2-EHA	$CH_2=CHCOOCH_2CH(C_2H_5)(CH_2)_3CH_3$	$CH_2=CHCOO\text{-}$, $CH_2CH(C_2H_5)(CH_2)_3CH_3$
PAANa	$[\text{-}CH_2\text{-}CH(CO_2Na)\text{-}]n$	$\text{-}CO_2Na$

Binder modification is important for the enhancement of the sintering and electrical properties of KNN-based ceramics. The functional group of PAA is the carboxyl group (-COOH), and its dissociation equation is $R\text{-}COOH+H_2O—R\text{-}COO^-+H_3O^+$. With the increase of pH value (4.5-5), the negatively charged carboxylic acid group (COO^-) formed by dissociation combines with K, Na, and Nb ions in KNN and agglomerates the powder by electrostatic attraction. However, if the amount of COO^- is excess, the granulated particle size becomes larger, and the particle fluidity turns worse, leading to uneven granulation. In addition, electrically neutral polymers or functional groups that are not sensitive to changes in pH value or ion concentration can shield the potential layer generated by partially ionized PAA to reduce unfavorable agglomeration and control particle size. Therefore, the alkalescence and neutral binders are theoretically supposed to possess better bonding properties and enhanced piezoelectric properties of corresponding ceramics. However, the KNN ceramics prepared with alkalescence PAA-DM, neutral PAA-C=CH_2, and PAA-2-EHA, are different. Based on their active groups, as shown in Table II, the COO^- is not well-shielded even if increased in these modified binders. The decreased piezoelectric properties of the PAANa are mostly ascribed to poor thermal decomposition performance. The reason for the optimized piezoelectric constant of the ceramic prepared by AcPAA is the good thermal analysis performance of AcPAA.

Moreover, since the maximum breakdown strengths are observed in alkalescent PAA-DM and neutral PAA-2-EHA, the conclusion that appropriately increasing the amount of COO^- is conducive to increasing the breakdown field strength, is drawn.

Conclusions

In this work, we investigated nine kinds of PAA-based binders and their effects on the electrical properties of corresponding ceramics. The results indicate that the optimized piezoelectric constants are obtained in alkalescent PAA-APAANa and acidulous AcPAA while the maximum breakdown strengths are observed in alkalescent PAA-DM and neutral PAA-2-EHA. The enhanced electrical properties contribute to the binding actions of the as-calcined KNN particles and the thermal decomposition performances of these binders, which are closely related to their structural formulas and active functional groups. Generally speaking, appropriately increasing the amount of COO^- is conducive to increasing the breakdown field strength. And the good thermal analysis performance gives rise to optimized piezoelectric constants of the ceramics. The ceramics synthesized by PAA-APAANa or AcPAA have the highest d_{33} of 103 or 108 pC/N, while the smallest d_{33} is detected for PAANa, which may be due to the low density. The maximum d_{33} of PAA-APAANa or AcPAA is attributed to the reduction of carboxylate groups ($-COO^-$) by regulating pH. In general, the KNN ceramics synthesized by AcPAA have the best-combined properties, with piezoelectric constants of $d_{33} \sim 108$ pC/N, while the breakdown strength of PAA-DM is ~ 3.93 kV/cm, which is attributed to the synergistic effect of particle size and thermal behavior of the adhesive.

Acknowledgment

This work was supported by the Guizhou University Student Innovation and Entrepreneurship Training Program, the Guizhou Provincial Basic Research Program (Natural Science) (No. ZK [2024] Key 020) and conducted under the joint guidance by the Tianjin University and Anzo Chemical Co. LTD. We also thank Prof. Wu in Sichuan University for the valuable suggestions with us.

References

1. Y. Tian, M.B. Gao, S.L. Xu, and M. Ye, China Powder Sci. Technol. 30[1] (2024) 66-78.
2. J.R. He, F.L. Sun, F.H. Han, J.J. Gu, M.R. Ou, W.K. Xu, and X.P. Xu, RSC Adv. 8 (2018) 12684-12691.
3. K.H. Didehban, L. Mohammadi, and J. Azimvand, Mater. Chem. Phys. 195 (2017) 162-169.
4. Y.G. Zhuo, J. Liu, F. Yang, Q.S. Li, and G.Z. Xing, Integr. Ferroelectr. 179[1] (2017) 166-172.
5. A.Y.S. Eng, D. Nguyen, V. Kumar, G.S. Subramanian, M. Ng, and Z.W. Seh, J. Mater. Chem. A. 43 (2020) 22983-22997.
6. Y. Wang, T.P. Wang, X.X. Jia, and C.S. Ye, J. Nucl. Sci. Technol. 60[2] (2022) 140-152.
7. D.H. Yao, J.W. Feng, J. Wang, Y.H. Deng, and C.Y. Wang, J. Power Sources. 463 (2020) 228188.
8. J.B. Lin, Y.Y. Hu, J.Y. Xiao, Y.X. Huang, M.Y. Wang, H.Y. Yang, J. Zou, B.L. Yuan, and J. Ma, Chem. Eng. J. 420 (2021) 129692.
9. J. Choi, K. Hwang, U. Kim, J. Lee, K. Shim, S. Kang, and W. Cho, J. Ceram. Process. Res. 20[5] (2019) 547-555.
10. J.H. Song, Z.H. Feng, Y. Wang, X.B. Zhou, X.H. Zhang, K. Wang, and J.Y. Xie, Solid State Ionics. 343 (2019) 115070.
11. C.J. Chen, Y. Deng, E.Y. Yan, Y. Hu, and X.Q. Jiang, Chin. Sci. Bull. 54 (2009) 3127-3136.
12. Z.G. Sun, H.Y. Shao, X.M. Niu, and Y.D. Song, Mater. Sci. Eng. A. 663 (2016) 78-85.
13. P.P. Rakesh Krishnan, P. Arun Kumar, and K. Prabhakaran, J. Rubber Res. 26 (2023) 291-301.
14. S.A. Uhland, R.K. Holman, S. Morissette, M.J. Cima, and E.M. Sachs, J. Am. Ceram. Soc. 84[12] (2001) 2809-2818.
15. S. Tanaka, C.C. Pin, and K. Uematsu, J. Am. Ceram. Soc. 89[6] (2006) 1903-1907.
16. Z.H. Wang, D.G. Ma, Y.H. Wang, Y. Xie, Z.G. Yu, J. Cheng, L. Li, L. Sun, S.X. Dong, and H. Wang, Adv. Sci. 10[17] (2023) 2207059.
17. W.F. Liu, L. Cheng, and S.T. Li, Crystals. 9[3] (2019) 179.
18. H.F. Liu, J. Zhao, H. Wang, Y.C. Zhu, J. Li, X.Q. Zhang, K. Zheng, and J.C. Huo, China Powder Sci. Technol. 28[3] (2022) 124-132.
19. J. Cho, Y. Lee, and B. Kim, J. Ceram. Process. Res. 11[2] (2010) 237-240.
20. L.M. Tan, X.C. Wang, W.J. Zhu, A.J. Li, and Y.Y. Wang, J. Alloy. Compd. 874 (2021) 159770.
21. J.H. Kim, K.W. Chae, and C.I. Cheon, J. Ceram. Process. Res. 23[5] (2022) 679-684.
22. G.X. Zhang, X.C. Wang, Q. Sun, Y.Y. Wang, and Q.L. Zhang, Ceram. Int. 48[18] (2022) 25996-26002.
23. P. Gao, X.Y. Huang, C. Liu, R.J. Zhang, X. Chen, P. Lei, F.P. Zhuo, and Z.H. Liu, J. Mater. Sci.: Mater. Electron. 34 (2023) 2210.
24. Y. Lakhdar, C. Tuck, J. Binner, A. Terry, and R. Goodridge, Prog. Mater. Sci. 116 (2021) 100736.
25. R. Pinho, A. Tkach, S. Zlotnik, M.E. Costa, J. Noudem, I.M. Reaney, and P.M. Vilarinho, Appl. Mater. Today. 19 (2020) 100566.
26. Y.Y. Wang, J.G. Wu, D.Q. Xiao, J.G. Zhu, P. Yu, L. Wu, and X. Li, J. Alloy. Compd. 462[1-2] (2008) 310-314.
27. A. Dinga and H. Wang, J. Ceram. Process. Res. 11[1] (2010) 44-46.
28. R.N. Xie, G.W. Zhang, X. Xiao, and Y. Long, China Powder Sci. Technol. 28[2] (2022) 106-113.
29. Y. Yu and B.Q. CAO, China Powder Sci. Technol. 29[6] (2023) 91-100.
30. X.Y. Zhang, Z.H. Ying, S.B. Guo, and W.L. Li, China Powder Sci. Technol. 30[2] (2024) 96-112.
31. M.U. Farooq, J.G. Fisher, J. Kim, D. Kim, E. Shin, Y. Kim, J. Kim, S. Moon, J. Lee, X. Lin, and D. Zhang, J. Ceram. Process. Res. 17[4] (2016) 304-312.